



**HAL**  
open science

# The Holocene sedimentary record of the flood plain of the Saint-Ciers-Sur-Gironde marsh (Gironde estuary, France)

Margret M. Ms Mathes-Schmidt, Denis Moiriat, Hervé Jomard, Klaus Reicherter, Stephane Baize

## ► To cite this version:

Margret M. Ms Mathes-Schmidt, Denis Moiriat, Hervé Jomard, Klaus Reicherter, Stephane Baize. The Holocene sedimentary record of the flood plain of the Saint-Ciers-Sur-Gironde marsh (Gironde estuary, France). *Zeitschrift für Geomorphologie, Supplementary Issues*, 2019, *Annals of Geomorphology*, 62 (2), pp.295 - 322. 10.1127/zfg\_suppl/2019/0605 . irsn-04220306

**HAL Id: irsn-04220306**

**<https://irsn.hal.science/irsn-04220306>**

Submitted on 27 Sep 2023

**HAL** is a multi-disciplinary open access archive for the deposit and dissemination of scientific research documents, whether they are published or not. The documents may come from teaching and research institutions in France or abroad, or from public or private research centers.

L'archive ouverte pluridisciplinaire **HAL**, est destinée au dépôt et à la diffusion de documents scientifiques de niveau recherche, publiés ou non, émanant des établissements d'enseignement et de recherche français ou étrangers, des laboratoires publics ou privés.



Distributed under a Creative Commons Attribution - NonCommercial 4.0 International License



## The Holocene sedimentary record of the flood plain of the Saint-Ciers-Sur-Gironde marsh (Gironde estuary, France)

Margret Mathes-Schmidt, Denis Moiriat, Hervé Jomard, Klaus Reicherter, Stéphane Baize

With 5 figures and 4 tables

**Abstract.** The Holocene sedimentary record of the flood plain of the Saint-Ciers-Sur-Gironde marsh was examined on sediment cores from the right bank of the Gironde estuary with regard to the evolution of the marsh and its potential to preserve high-energy deposits. Sedimentological, geochemical, geophysical and micropaleontological methods were applied. Radiocarbon ages in the central part of the investigation area reach back to  $7,971 \pm 44.5$  BP. The sediments of the Saint-Ciers-sur-Gironde marsh reflect the conditions of a Holocene estuarine salt marsh before human activity and draining. The interpretation of the core data showed that the study area includes different facies during development from the pre-Holocene to recent times: tidal mudflats in the northwest at Mortagne and Beaumont, and a fluvial facies developing into an estuarine facies in the southeast near Camp and Saint-Ciers-Sur-Gironde. The last stage is the formation of the saltmarsh. The changes in grain size reflect different transport mechanisms during the development from a fluvial environment to the recent marsh. First gravel, then sand and finally muddy sediments were deposited in the estuary and finally in the marsh area. Below the salt marsh deposits in Mortagne-Sur-Gironde, there is some evidence of deposits from energy-rich events in tidal mudflats. The southern and central part, in which estuarine clays were deposited, was probably most of the time outside the range of storms. On the marshland surface, erosion, pedogenesis and bioturbation processes destroy storm relevant layers in a very short time.

**Keywords:** Saint-Ciers-Sur-Gironde marsh, Holocene, estuary development, high-energy events

### 1 Introduction

During the extratropical cyclones “Lothar” and “Martin” in December 1999, flooding of the nuclear power plant “Blayais”, situated at the right bank of the Gironde estuary, resulted in an automatic shut down of two reactors accompanied by the failure of the emergency water pumps (GORBATCHEV et al. 2001). After the incident, the dams near the power plant were raised to 8 m (SALOMON 2002). The low elevation of the marsh (below 2.5 m NGF – nivellement générale de la France) makes its surface prone to flooding events on a regular seasonal basis. Floods in the Gironde estuary are caused not only by the increased flow of the Garonne and Dordogne rivers, but also by storm surges from the Atlantic Ocean. If meteorological events (like storms and heavy rainfall) concur with storm tides, water levels in the estuary can reach heights of 7 m NGF and above (SALOMON 2002).

We focused on the east bank of the estuary as this area was flooded in 1999 around the nuclear power plant. The study area includes large parts of the salt marsh of the Gironde estuary called the Saint-Ciers-sur-Gironde marsh (hereinafter referred to briefly as St.-Ciers marsh), the largest marsh area of the east bank formed by the widening of the main channel (Fig. 1). We studied the sedimentary record of the Holocene flood plain in order to understand the evolu-

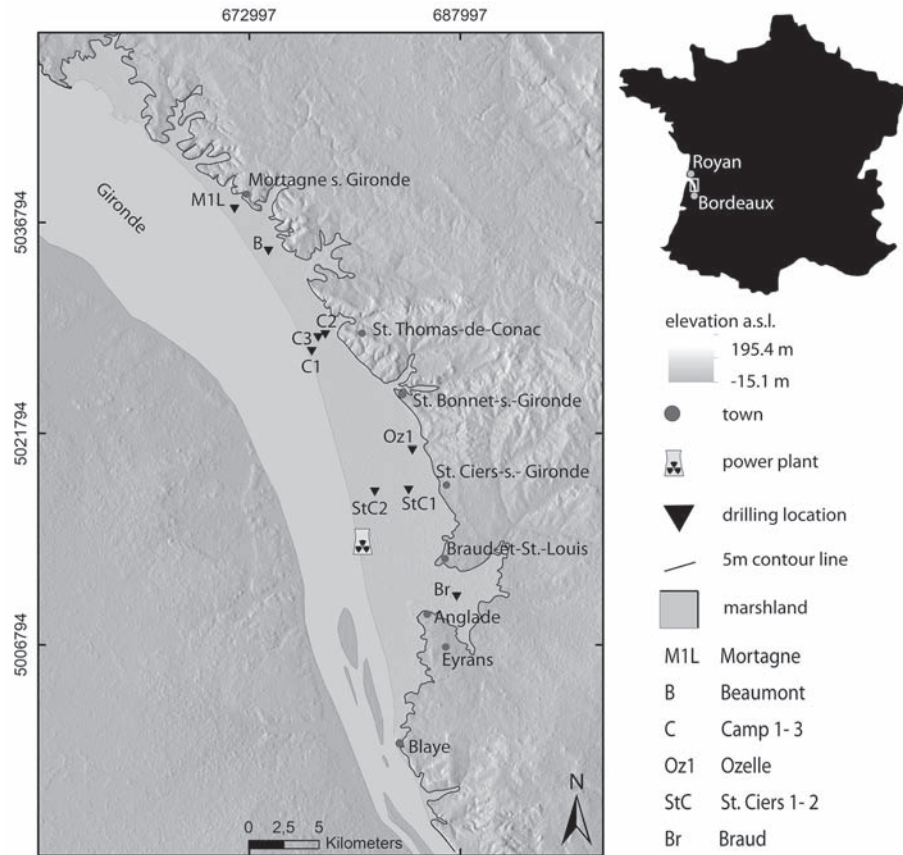


Fig. 1. The St Ciers marsh at the eastern bank of the Gironde estuary with drilling sites. The 5 m contour line illustrates the extent of the march. Coordinates in UTM, topography based on the U.S. GEOLOGICAL SURVEY (2014, 2017).

tion of the marsh, the past depositional processes and to reconstruct the paleoenvironment over time. This includes the detection of potential high-energy event deposits, the preservation of which is strongly dependent on the paleoenvironment. In addition, the distribution of storm-related sediments is of interest for a more accurate assessment of the influence of storms in the Gironde estuary. A drilling campaign was therefore carried out in March 2013 with subsequent laboratory analyses.

## 2 Investigation area

The study area is located in the northwestern edge of the Aquitaine Basin which is confined to the north by the Massif Americain, to the northeast by the Massif Central and to the south by the Pyrenees (DOUBREUILH et al. 1995). Upon the Variscan basement lies a mostly less than 3 km thick Mesozoic – Cenozoic cover (BITEAU et al. 2006). Tectonic compression and the as-

sociated uplift of the basin (PLATEL 1987) led to a marine regression from the late Cretaceous to early Palaeogene. The St.-Ciers marsh measures 30 km in length from its northern edge near Mortagne-sur-Gironde to its southernmost part and covers an area of 400 km<sup>2</sup> (Fig. 1). It is bounded in the west by dams and in the east by low hills that turn into 15 m high cliffs of Cretaceous chalky limestones (Campanian) near Mortagne-Sur-Gironde. From St. Bonnet-sur-Gironde towards the south the boundary of the marsh is formed by continental sand and clay deposits of the Eocene (Lutetian). The marsh surface lies between 0.5 m and 2.5 m NGE, while the highest embankments are 8 m high (SALOMON 2002). The recent rate of subsidence is assumed to be 0.2 mm to 0.5 mm per year. (RISKSNAT.ORG 2001). The marsh is described as an estuarine back-barrier type salt marsh (ALLEN 2000). Most of the area is used as grassland and farmland, therefore it is burred by a dense net of draining channels.

The Gironde estuary is the largest in western Europe and perhaps the best investigated in all its sections (eg. CASTAIGN & ALLEN 1981, JOUANNEAU & LATOUCHE 1981, ALLEN & POSAMENTIER 1993, PONTEE et al. 1998, MELLALIEUX et al. 2000, COQUILLAS 2004, BILLY et al. 2012). The estuary has an extent of c. 635 km<sup>2</sup> and reaches from the confluence of the Dordogne and Garonne rivers near Bordeaux (Bec d'Ambès) to the Atlantic Ocean at a distance of 75 km (MUIR 2013, JOUANNEAU & LATOUCHE 1981). The catchment area extends over an area of 75,000 km<sup>2</sup> (ALLEN & POSAMENTIER 1993).

### 2.1 *Hydrology and sedimentology of the estuary*

The Gironde estuary was formed during the Holocene sea level rise and belongs to the drowned river valley type (PRITCHARD 1967, ALLEN & POSAMENTIER 1993). The Gironde is defined as a mixed energy (wave- and tide-dominated) meso- to macrotidal estuary (DALRYMPLE et al. 1992, ALLEN & POSAMENTIER 1993, MELLALIEUX et al. 2000, KAPSIMALIS et al. 2004, LARROSE et al. 2010) and is regarded as relatively mature, as it has already filled its corresponding drowned Holocene river valley to a large extent (CASTAIGN & ALLEN 1981). The St.-Ciers-marsh (Fig. 1) developed on the right bank of the mid-estuary which is more tidal dominated (KAPSIMALIS et al. 2004).

Since the beginning of the 20<sup>th</sup> century, reliable data have been collected on fluvial discharges, which are most likely under anthropogenic influence. The mean combined discharge of the Garonne and Dordogne rivers into the Gironde for the years 1990 to 1999 is about 1100 m<sup>3</sup> s<sup>-1</sup> (SCHÄFER et al. 2002), but can reach peak values of up to 3000 m<sup>3</sup> s<sup>-1</sup> during the flood season (JOUANNEAU & LATOUCHE 1981). SCHÄFER et al. (2002) estimate annual river water flux into the Gironde to be about  $34 \times 10^9$  m<sup>3</sup> year<sup>-1</sup>. The total influx of fluvial sediment into the Gironde varies between 2 and 4 Mt year<sup>-1</sup> (MIGNIOT 1971, SCHÄFER et al. 2002), while the output is estimated to be 1.2–1.5 Mt year<sup>-1</sup> (LESUEUR et al. 2002).

The sediment load consists of 75 % of silts and clays, while the remaining 25 % predominantly consists of sand (MIGNIOT 1971). The total amount of suspended sediment in the estuary is obtained from fluvial sources (CASTAIGN & ALLEN 1981, ALLEN 1973). Marine, sandy sediments are deposited only as a few hundred thousand m<sup>3</sup> year<sup>-1</sup> near the mouth (ALLEN et al. 1979). Sediment transport takes place in suspension for particles < 60 µm and as bedload for particles > 60 µm (JOUANNEAU & LATOUCHE 1981). Sedimentation rates are highest on the east-

ern bank and in the central, low-energy part of the estuary during neap tide slack water periods (CASTAIGN & ALLEN 1981, AGENCE DE L'EAU 1994, ROBERT et al. 2004) whereas erosion occurs at mid-ebb and mid-flood (ROBERT et al. 2004).

The estuary is strongly influenced by the Atlantic tides (FENIES & TASTET 1998, GHAIN et al. 2014) with tidal ranges between 1.5 m for neap tides and 5.5 m for spring tides (MELLALIEUX et al. 2000). The mouth of the Gironde estuary leaves a 23 km wide gap in the 10 m –15 m high dune belt that stretches along this part of the French Atlantic coast. The estuarine funnel is restricted to an approx. 5 km wide opening between the Pointe de Grave to the south and the town of Royan to the north. The shallowing of the inlet acts as a coastal barrier and thus strongly reduces tidal energy by friction (YANG et al. 2006). The wide funnel shape of the estuary is able to equalise river floods to a certain extent, but mainly leads to an upstream enhancement of marine flooding (SALOMON 2002).

In most cases of severe flooding, strong winds came from a NW direction and thus right along the axis of the estuary (SALOMON 2002). Wind waves inside of the estuary are, under normal conditions, considered relatively weak due to a small wind fetch. But during the storm in December 1999 waves piled up to 2 m height within the estuary (SALOMON 2002). For cyclones such as “Lothar” and “Martin” in December 1999a return time of almost 200 years is expected, but this prognosis is highly dependent on the current mean sea level (VAN DER MEER et al. 2005).

## **2.2 Evolution of the Saint-Ciers-sur-Gironde Marsh**

### **2.2.1 Pre-Holocene – phase A (15,000 BP –13,000 BP)**

During the Lower Pleistocene alluvial and fluvial sediments were deposited on the Eocene bedrock (DOUBREUILH et al. 1995, JOUANNEAU 1973). From about 18,000 BP onwards, the incised Gironde Valley was flooded due to rising sea levels (ALLEN & POSAMENTIER 1993, PONTEE et al. 1998). Between c. 15,000 BP and 13,000 BP, sea level was about 70–80 m below today's sea level (LAMBECK 1997, SIDALL et al. 2003, LAMBECK et al. 2014, HARFF et al. 2017), and remained relatively stable. Incision into Eocene and Cretaceous substratum ended and deposition of a first layer of pebbles and gravel commenced (JOUANNEAU & LATOUCHE 1981). The Gironde valley had a steep slope and coarse sand and gravel from a periglacial braided river system covers the ancient thalweg (JOUANNEAU & LATOUCHE 1981).

### **2.2.2 Late Pleistocene to early Holocene – phase B (13,000 BP –6,000 BP)**

From about 13,000 BP to c. 6,000 BP the sea level rose rapidly to c. 2 m –5 m below the present sea level (KIDSON 1982, ALLEN 2000, SIDALL et al. 2003, LAMBECK et al. 2014, HARFF et al. 2017). The study area was affected by the depositional influence of a meandering channel. Grey, medium to coarse sands with occasional fine gravels and high mud contents were mostly deposited near the channel in the form of alluvial ridges or hinter-marshes. After COQUILLAS (2004), as soon as the estuary has developed a certain width, the interaction of main channel and counter-flow near the right bank leads to the deposition of large amounts of sediments in the shearing area. Small islands and shoals connected and formed a barrier which led to the formation of a

protected lagoon that later became the St.-Ciers marsh. The lowermost estuarine muds are not yet dated, but if assumed sedimentation rates of MELLALIEU et al. (2000) are extrapolated, the mud deposition started around 10,000 BP.

JOUANNEAU & LATOUCHE (1981) mention a regressional phase shortly after deposition of the first estuarine muds, characterised by deposition of sand and gravel on top of the first mud layer and after KIDSON (1982) there is at least one major episode of stagnation or even regression between 10,000 BP and 6,000 BP. For the Gironde, it is very likely that temporary stagnation in the relative sea level rise resulted in a rapid salt marsh growth (JOUANNEAU & LATOUCHE 1981).

### **2.2.3 Late Holocene phase C (6,000 BP – Present)**

Today's sea level was reached around 6,000 BP (LAMBECK 1997, PONTEE et al. 1998), around 4,000 BP after SIDALL et al. (2003). Approximately at 4,000 BP to 6,000 BP fluvial sediment supply exceeded accommodation space, leading to the formation of the first salt marshes and tidal flats on the flanks of the estuarine channel (PONTEE et al. 1998). Peat layers developed mainly between 6,000 BP and 2,200 BP. No reliable accretion rates were calculated as unknown parameters like compaction, peat growth and marsh maturity erosion would have been to be considered (MELLALIEU et al. 2000). The final phase of estuarine infilling in the marsh interior was characterised by a much slower rise of the sea level with only minor fluctuations (FAIRBRIDGE 1961, KIDSON 1982).

### **2.2.4 Anthropogenic influence**

The oldest findings of human presence date back to Neolithic times (8,000 BP – 3,750 BP) and were found on the top of the limestone cliffs and along the marsh margins. The first significant settlements are known from the iron age (2,675 BP – 2,000 BP) (MELLALIEUX et al. 2000). Since 1654 AD the marsh has been protected from the sea by embankments (MELLALIEUX et al. 2000). Initial dredging of the main navigation channels started around 1850 (JOUANNEAU & LATOUCHE 1981). Before this human intervention in the riverbed, the development of the estuary can be described as natural (AGENCE DE L'EAU 1994). Long-term settlement may be responsible for the development of the estuary and the marsh (RISK NAT.ORG 2001) just as for the inundation by high tide, flood water and storms. Embankments along the St.-Ciers marsh have been improved after severe flooding in 1952 (VAN DER MEER et al. 2005) and local citizens (March 2013) told of the end of frequent flooding of the marsh about 50 years ago. The current dams are between 3.50 m and 5.50 m high; only in close proximity to the Blayais power plant they were elevated to 8 m after flooding in 1999 (SALOMON 2002). Today the study area is cut off from the estuary by dams and the recent surface is used as farmland.

## **3 Methods**

In March 2013 we drilled 12 boreholes at different sites (Fig. 1) to a maximum depth of 13 m using an Altas Copco portable jackhammer and an open window sampler with an inner diameter of 50 mm. At 3 sites we drilled a second borehole with PVC-Liners 1 m in length and 5 cm in diameter (Table 1). A total of 88 m were drilled, 15 m of them in PVC-liners. The drilling sites

Table 1. Borehole locations from north to south and laboratory investigations. Here core loss is not considered in core and liner length.

No.	Coordinates (GPS)	core length	PVC-Liner	Height	Surface	Laboratory investigations
	UTM	[m]	[m]	[m a.s.l.]		
Mortagne1		5.00		2.00		
Mortagne1L (M1L)	30T E48.005 N5037769	6.00	6.00	2.00	Pasture, 50 m E of large tidal channel and ancient dike	XRF, micropaleontology, magnetic susceptibility, grain size analysis
Beaumont (B)	30T E674366 N5034780	6.00		3.00	Pasture, 30 m E of dike	micropaleontology
Camp1 (C1)	30T E677449 N5027643	13.00		3.00	Farmland, ploughed	Micropaleontology, Radiocarbon dating
Camp2 (C2)	30T	6.00		2.00	Pasture, 10 m N of small channel	
Camp2L (C2L)	E678406 N5028838	5.00	3.00	micropaleontology, XRF, grain size analysis		
Camp 3 (C3)	30T E679198 N5028544	6.00		3.00	Farmland, soil remnants	Micropaleontology, radiocarbon dating
Ozelle (Oz1)	30T E684242 N5020641	3.00		1.50	Road embankment	Grain size analysis, micropaleontology
St.Ciers1 (StC1)		8.00		1.00	Road embankment, 10 m SE of a pond	Grain size analysis
St.Ciers1L (StC1L)	30T E684242 N5020641	6.00	6.00	1.00		Magnetic susceptibility, grain size analysis, micropaleontology
StCiers2 (StC2)	30T E681895 N5017651	6.00		0.50	Farmland, ploughed	Grain size analysis
Braud (Br)	30T E687758 N5010250	11.00		1.00	Road embankment, swamp	
Total		73.00	15.00			

are located in shallow depressions that had been flooded in recent centuries. The sediment cores were examined with regard to stratigraphy, colour (Munsell colour chart), sedimentology (such as grain size, internal structures, etc.), plant and fossil remains, photographically documented and representative layers sampled. Grain size analysis, measurement of magnetic susceptibility, quantitative and qualitative element distribution, micropaleontological investigations and radiocarbon dating (Table 1) were used to distinguish the often homogeneous sediments.

### ***Grain size***

Grain size analysis was done by sieving and laser granulometry depending on the sample properties. Samples from sandy and gravelly horizons of the open window samplers and the liners underwent sieve analysis. After drying at the low temperature of 40 °C to preserve the organic matter, the samples were sieved wet with a RETSCH AS 2000 and then dried again at 40 °C. According to DIN 18123 (1996), sieves with the following diameters were used: 4 mm, 2 mm, 1 mm, 0.5 mm, 0.25 mm, 0.125 mm and 0.063 mm.

Samples of silt or sub-silt grain size were determined by laser-granulometry carried out with a Beckmann Coulter LS 13 320 Laser Diffraction Particle Size Analyzer at the laboratory of the Physical Geography and Geoecology of the Department of Geography, RWTH Aachen University. If the clay content of a sample was about 20 %, 10 g –20 g materials were homogenized. Larger particles were sieved out, external plant remains like stems and roots were picked out as well. Different preparation steps with distilled water, hydrogen peroxide, heating and treatment with natriumpyrophosphate solution were used to remove organic materials and disaggregate grains. We dismissed the use of HCl to remove carbonate concretions as they were regarded as an elementary component of sediment facies. This also applies to organic material partially, but a difference had to be made between particles co-deposited with mineral grains from the particulate suspended material of the estuary and extraneous debris, such as roots or stems from peat above or soil below the layer to be examined. The laser granulometry used a 5mW diode at a wavelength of 780 nm. The PIDS system (Polarization Intensity Differential Scattering) was activated to include particles of sizes smaller than 1 µm –0.04 µm. Runs were determined with portions of 0.10 g and 0.15 g.

Mean, median, skewness (asymmetry of grain size distribution), standard deviation (sorting) and kurtosis (peakedness of grain size frequency curves) have been calculated using the formulas of FOLK & WARD (1957) and are presented in three different diagrams. The CM-diagram after PASSEGA (1957, 1964) and PASSEGA & BYRAMJEE (1969) allows to determine the kind of sedimenttransport. Originally the CM-diagram deals with marine environments but further investigations showed the applicability to fluvial systems (PASSEGA & BYRAMJEE 1969, BRAVARD & PEIRY 1999, SALVADOR et al. 2005, MYCIELSKA-DOWIGIAŁŁO & LUDWIKOWSKA-KĘDZIA 2012, BRAVARD et al. 2014). The plot of mean vs sorting after TANNER (1991) shows sedimentation areas of coastal environments including estuarine areas. The diagram using skewness vs kurtosis after FOLK & WARD (1957) (Fig. 4, A–D) shows deviations from the normal distributions and allows the distinction between the sediments.

### ***X-ray-fluorescence (XRF)***

Quantitative and qualitative element distributions of Ca, Sr, Fe, Ti and K were determined via portable X-ray fluorescence analysis using a field portable NITON XLt 700 equipped with a silver transmission target and a solid state detector. It was measured at 1 cm intervals with a measurement time of 30 seconds. The elements Ca, Sr are used as indicators for marine environments (DICKSON & GOYET 1994) while Fe, Ti delivered by detritus and pedogenesis were used as terrestrial indicators (SAGEMAN & LYONS 2003) and K as part of illite and smectite which are abundant in clays of the Gironde area (GRANBOULAN et al. 1989).

### ***Magnetic susceptibility (MS)***

Measurements were made with a MS2 from Bartington Instruments with MS2K sensor and a 2 cm spacing on the open, cleaned PE-liner. The calibration of the sensor was carried out with the standard provided with the instrument. MS allows the differentiation of minerals by their magnetizability, particularly Fe-bearing minerals (DEARING 1999).

### ***Micropaleontology***

Micropaleontological investigations were performed with the residues of the grain size analyses. To minimize the effect of sample contamination the sieves were treated with methylene blue before each sieving process. Additional clay-rich samples were treated with 5 % hydrogen peroxide (H<sub>2</sub>O<sub>2</sub>) to take off clay cover. The main focus was laid on foraminifera. Diatoms, ostracodes and other bioclasts are mentioned without a classification of species or taxa. Due to the low amount of microfossils ( $\leq 60$  foraminifera per 20 g sample weight), only a qualitative and semiquantitative evaluation was possible.

### ***Radiocarbon dating***

Radiocarbon dating (Table 2) of samples from two cores were performed at the LMC 14/LSCE Orsay laboratory. The obtained ages were calibrated using the oxcal software (BRONK RAMSEY 2009) and the Northern Hemisphere calibration curve IntCal13 (REIMER et al. 2013).

Table 2. Radiocarbon dates from C1, C3 (calibrating: oxcal software, BRONK RAMSEY, 2009, Northern Hemisphere calibration curve IntCal13, REIMER et al. (2013) and *samples in italic* from MEL-LALIEUX et al. (2000).

Core/liner depth	Sample reference	Material	mg C	Delta C13	pMC	Conv. Age (a BP)	mean cal yrs BP
C1 12.69 – 12.76 m	NUG-1	Clay with plant remains	1.513	-27.0	41.168 ± 0.176	7,130 ± 35	7,971.5 ± 44.5
C1 5.42 – 5.51 m	NUG-2	peat	0.291	-29.1	49.292 ± 0.234	5,685 ± 40	6,484 ± 8 6
C3 5.36 – 5.43 m	NUG-3	clay with plant remains	1.188	-27.4	46.551 ± 0.173	6,140 ± 30	7,055.5 ± 103.5
C3 3.80 – 3.86 m	NUG-4	clay with plant remains	0.187	-30.6	55.974 ± 0.224	4,660 ± 30	5,392 ± 77
<i>HO 9607 – 350–355 cm</i>	<i>Beta 99067</i>	<i>peat</i>					5,770 ± 155
<i>HO 9608 – 311–316 cm</i>	<i>Beta 99068</i>	<i>peat</i>					4,470 ± 145
<i>HO 9611/12 – 210–215 cm</i>	<i>Beta 104801</i>	<i>peat</i>					6,422 ± 132

## 4 Results

### 4.1 Mortagne IL (MIL)

#### *Lithology*

From the total depth of 5.38 m to 1.45 m, the sediment core consists of alternating sections of homogenous dark-grey mud and laminated silty-sandy mud (Fig. 2). The homogenous layers contain rare shell fragments and disarticulated as well as articulated *Scrobicularia* in different amounts and sizes ranging from few mm to 2 cm. Abundant micas, charcoal and few solitary sand grains are found but do not follow a particular distribution pattern. The homogenous mud also contains very few silty to sandy layers of less than 0.5 cm thickness, especially near the contacts to laminated silty-sandy mud. Laminated silty-sandy mud occurs in three intervals of upward increasing thickness. Contacts to the homogenous mud are sharp for the lowest, but fluent for the uppermost layer. The laminations are mostly, planar, rarely oblique or slightly undulated and vary in thickness from almost 1 cm to less than 1 mm. Distinct calcified bioturbation and root penetration are present from 2.21 m to 1.46 m depth. This succession is covered by c. 1.00 m of a brown compacted mud.

#### *Micropaleontology*

Mikrofossil samples were taken from homogeneous dark-grey mud and laminated silty-sandy mud intervals. Twelve genera and eight species were identified. *Ammonia tepida*, *Haynesina germanica* and *Trochammina inflata* are the most abundant species in nearly all samples (Table 3). *Cibicides lobatulus*, *Planorbis mediterranensis*, reworked *Globigerina* sp (possibly from the Cretaceous) and *Bolivina* sp. occur less abundant. Furthermore, *Lagena*, sp./*L. striata*, *Milionella subrotunda*, *Fissurina orbignyana* and *Bulimina* sp. were found, all common on the shelf (table 3). Diatoms occur in all samples; ostracods, siliceous sponge spicules, spines of sea urchins and juvenile bivalves with numerous exemplars are present in most of the samples (Table 3).

### 4.2 Beaumont

The sediment core (Fig. 5) consists of homogenous dark-grey mud between 5.50 m and 1.50 m depth and is covered by brown compacted mud with carbonate concretions (diameter  $\leq 1$  cm). The dark-grey mud has largely the same composition as in the MIL, with the difference that shell fragments are much rarer and smaller, microfossils are completely absent. Silty-sandy laminae are also less abundant and occur mainly in the upper two meters of the homogeneous dark grey mud. The organic content is very high throughout the core and consists mainly of small plant fibres, charcoal and mineralised residues of roots and stems. Fe-mineral precipitations often occur in the form of mm-sized black nodules and striations.

### 4.3 Camp

About 10.6 m homogeneous blue-grey mud (13.0 m –2.27 m) was drilled in C1 (Fig. 5), which contains two peat intervals (8.25 m –8.18 m, 5.43 m –5.49 m) with up to 5 cm long macerated reed stems. Further, smaller, reddish brown peat lenses decrease towards the top and between

Table 3. Foraminifera and microfossil content of the Mortagne 1L borehole sorted by frequency of findings and their preferred habitat after (1) HOFKER 1977, (2) ALAVI 1988, (3) DEBENAY et al 2000, (4) DEBENAY & Guillou 2002, (5) FIORINI 2004, (6) DUCHEMIN et al 2005, (7) DUPUY et al. 2010, (8) HAYWARD et al. 2006,

		<i>Haynesina germanica</i>	<i>Ammonia tepida</i>	<i>Trochammina inflata</i>	<i>Haynesina</i> sp.	<i>Cibicides lobatulus</i>	<i>Globigerina</i> sp. reworked	<i>Ammonia</i> sp.	
	preferred habitat	intertidal mudflats, estuarine	intertidal mudflats, estuarine, suboxic	intertidal mudflats, estuarine, marsh	inner shelf marsh	subtidal, tidal flat, infralitoral,	planctic	subtidal - tidal flat	
	references	4, 9, 11	1, 3, 4, 5, 7, 15	1, 4, 5, 9, 11, 12	10	1, 5, 10, 11		4, 10	
Sample / depth in cm blg	sediment								
M1L / 243-251	laminated silty sandy mud	xxx	xxx		xx			xxx	
M1L / 306-315	homogeneous dark grey mud	xxx	xxx	xx	xxx	x	x	xxx	
M1L./ 320-329	homogeneous dark grey mud	xx	xx	xx					
M1L / 336-343	laminated silty sandy mud	xxx	xx	xxx		x			
M1L / 351-360	laminated silty sandy mud	xxx		x	x		x		
M1L / 362-370	laminated silty sandy mud	xx	xxx		x	x	x	x	
M1L / 375-382	homogeneous dark grey mud	x				x		x	
M1L / 382-390	homogeneous dark grey mud	xxx	xxx	xx			xx		
M1L / 408-416	homogeneous dark grey mud	xxx	xxx	x	x		xx		
M1L / 432-440	laminated silty sandy mud	xxx	xxx	x	xx	xxx	xx	x	
M1L / 466-475	homogeneous dark grey mud	xxx	xxx	xx	x	x			
M1L / 487-495	homogeneous dark grey mud	xx	x	x	x	x	x		
M1L / 512-521	homogeneous dark grey mud	xxx	xx	xxx	x	xxx			

5.43 m and 2.40 m the blue-grey mud is very homogeneous. From 7 m upwards, isolated shell fragments ( $\leq 1$  mm) occur, while microfossils are completely absent. A peat layer (2.4 m – 2.27 m) forms the transition to brown, compacted mud. For calibrated radiocarbon ages see Table 2 and Fig. 5. Both cores, C2 and C2L, were taken from the same site, but the liner core of C2L (Fig. 3) does not begin until 2 m depth. The basal parts of the sediment cores C2 (6 m – 1.38 m) and C2L (5 m – 3.27 m) consist of homogeneous blue-grey mud with small peat lenses and thin layers of

(9) HORTON & EDWARDS 2006, (10) MURRAY 2006, (11) HORTON & MURRAY 2007, (12) HAYWARD et al. 2010, (13) KOHO & PIÑA-OCHOA 2012, (14) HOLBOURN 2013, (15) THIBAUT DE CHANVALON et al. (2015).  
 x = rare, xx = common, xxx = abundant.

	<i>Bolivina</i> sp.	<i>Miliolinella subrotunda</i>	<i>Planorbina mediterraneensis</i>	<i>Lagena</i> sp., <i>L. striata</i>	<i>Fissurina orbignyana</i>	<i>Bulinina</i> sp.	ostracods	Sponge spicule	spines of sea urchins	diatoms
	shelf, silt, clay	continental shelf	shelf	shelf	inner shelf	lower neritic - bathyal, silt, clay	marin - brackish	marin	marin	marin - brackish
	2, 4, 10	6, 10	10	6	12, 14	2, 10, 14,				
	x		x			x	xxx		x	xx
		x	x				xx	xxx		xxx
							xx	x	x	xx
	xx		x		x		xxx	x	xxx	xxx
	x			x			x	x	x	xxx
										xxx
		x					x	x	x	xxx
	x			x			xxx	xx	xxx	xx
	x		x				xxx		xxx	xx
		xx	x				xx	x	xxx	xx
				x	x		xxx	x		x
							x	x	xxx	xxx
	x	x				x	xxx	x		x

dark, organic, rich mud with Fe<sup>3+</sup> / Mn<sup>3+</sup> mineralizations. Peat layers occur at 1.98 m –1.85 m and 4.4 m –4.3 m (C2) and 4.55 m –4.51 m (C2L), respectively. The homogeneous blue-grey mud is overlaid by the brown compacted mud. Muddy and sandy intervals in the blue-grey mud (C2, C2L) and in the brown-compacted mud contain hardly any microfossils apart from a few diatoms, ostracods and very rarely foraminifers (bolivinoids, buliminoids, reworked *Globigerina*). Reference samples from the surface of the marsh also contained no microfossils.

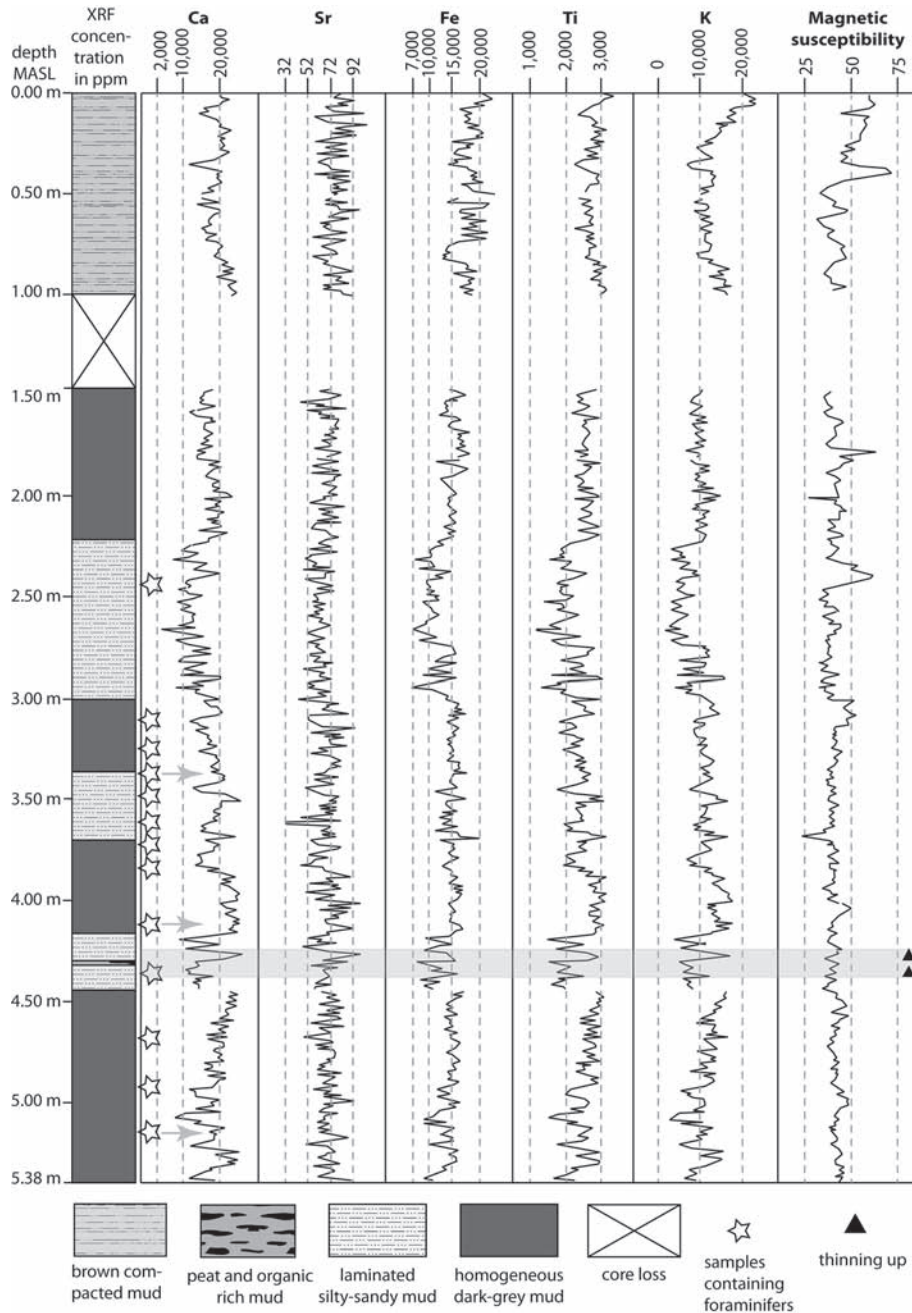


Fig. 2. Drilling profile MIL with XRF and magnetic susceptibility results. Discontinuities in the measured values are associated with the start of a new liner. Grey arrows mark microfossil samples that may be associated with paleostorms (see discussion of paleostorm evidence).

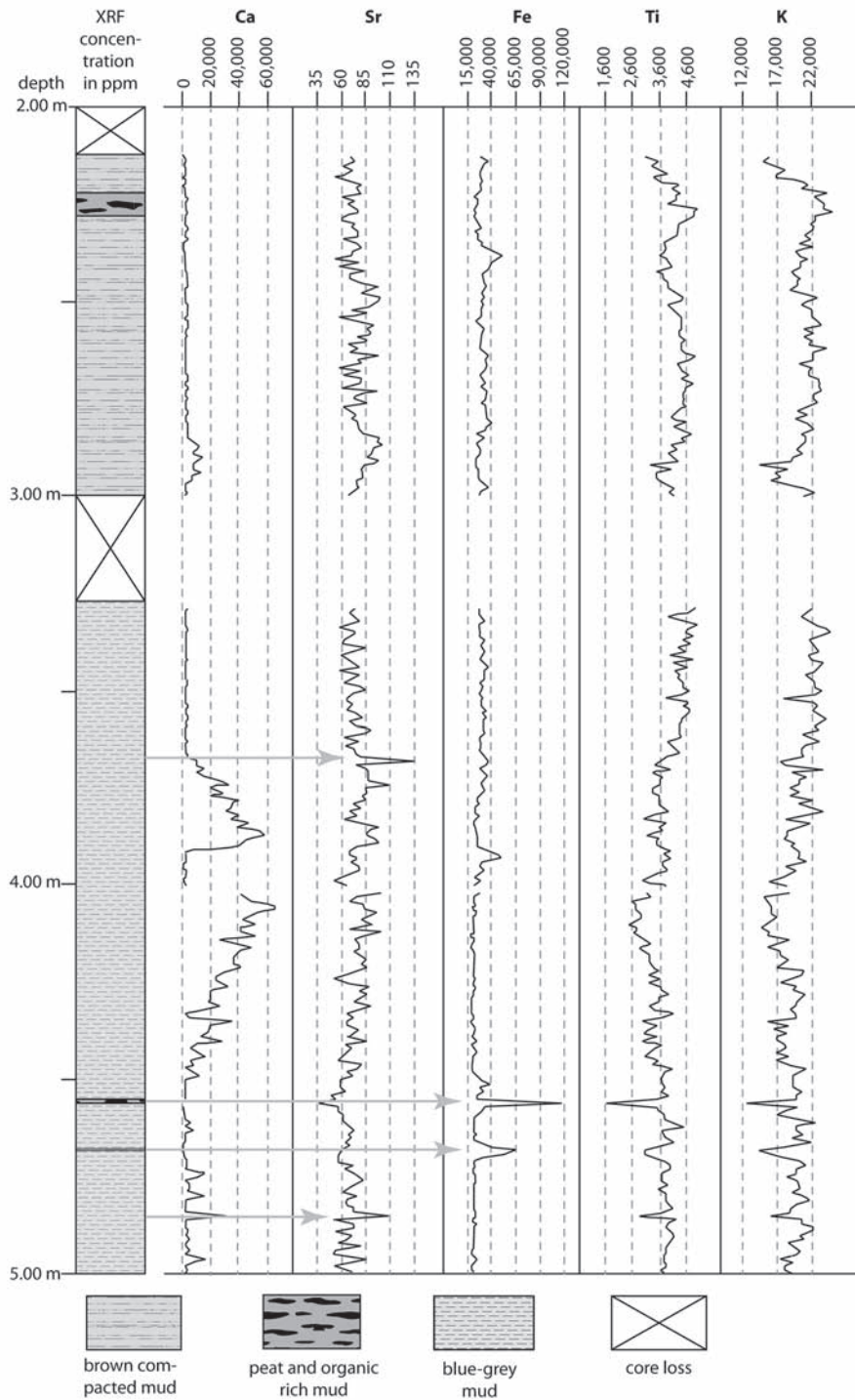


Fig. 3. XRF results of C2L plotted against depth. Discontinuities in the measured values are associated with the start of a new liner. Grey arrows mark layers with high Sr values and low K values respectively peat layers with clearly negative correlation of Sr and Fe.

In C3 (Fig. 5), from a final depth of 6 m to 2.65 m, very homogeneous blue-grey mud with only a few plant remains was drilled. After a 10 cm thick layer of black, carbonaceous plant material with high mud content (2.55 m – 2.65 m), brown compacted mud occurs with many carbonate concretions ( $\varnothing$  approx. 1 cm) and abundant  $\text{Fe}^{3+}$  /  $\text{Mn}^{3+}$  mineral precipitations. This core is free of fossils over its entire length. The calibrated radiocarbon ages can be taken from table 2.

#### 4.4 *StCiers*

The undisturbed sediments below the anthropogenic material were reached at 0.75 m (StC1), 0.87 m (StCIL), respectively (Fig. 5). The basal sediments of core STC1 (7.9 m – 6.76 m) and StCIL (7 m – 5.42 m) consist of moderately sorted, fine and medium sand with well rounded grains and gravel. The sand is covered by very homogeneous blue-grey mud up to 1.56 m bgl. Intercalated, thin layers with fibrous plant remains and dark brown peat lenses are often characterised by a distinct smell of hydrogen sulphide ( $\text{H}_2\text{S}$ ). The blue-grey mud is overlaid by a peat layer (from 1.1 m in STC1, from 1.50 m in STCIL upwards), which is cut off at the top by anthropogenic filling. The peat has a magnetic susceptibility  $\leq 5$  while the blue-grey mud has an average magnetic susceptibility between 5 and 70. In some horizons the plant material is completely replaced by Fe minerals. In this case the magnetic susceptibility is significantly higher than in plant rich and peaty layers. With the exception of diatoms and rare sponge needles, microfauna is absent in depths below 4 m.

The sediment core StC2 (Fig. 5) consists between 6 m and 1.0 m of a very homogeneous blue-grey mud with only a few dark brown peat lenses. To a depth of 0.62 m, this is covered by humified, dark brown peat with few small plant remains. The uppermost layer (0.62 m to 0.18 m) consists of clayey mud with large amounts of plant remains.

#### 4.5 *Ozelle 1 (Oz1)*

From a total depth of 3.0 m to 2.70 m, light yellow, very poorly sorted, coarse sands appear, overlaid by grey, poorly sorted, medium to fine, well rounded gravel, which is composed of quartz, quartzite and rare flint. From 2.20 m to 1.26 m depth alternating bedding of muddy peat and dark-grey, well sorted, medium sands is observed. In this interval also two individual layers of peat occur. All sand units in Oz1 show a medium to high mud component that does not exceed 10 %. The uppermost horizon in the Oz1 core (1.26 m – 0.37 m, core loss 0 – 0.37 m) is built of rooted, muddy, well humified dark brown peat with mud contents around 50 % and brownish grey organic rich mud (Fig. 5).

#### 4.6 *Braud (Br)*

The southernmost drilling, Br (Fig. 1), is located in a swampy area 3 km southeast of Braud-et-St.-Louis near an artificial dam of gravel and coarse sand which contaminate the whole core by caving material. From 3.50 m to total depth at 11 m depth blue-grey mud occurs. Large plant remains within are concentrated in 2 cm – 10 cm thick layers, occurring in irregular intervals and only in the deeper part of the core (7 m to 9 m, Fig. 5). The peat horizon from 3.50 m to 1.90 m is comparable to that of Oz1. It is comprised of 30 % – 40 % black organic-rich mud and moder-

ately humified peat consisting mainly of reed stems and leaves. A layer of homogenous dark grey mud containing small plant remains and few organic-rich streaks as well as Fe-mineral precipitations follows from 1.90 m to 1.42 m. Very poorly sorted, coarse sand from 1.42 m depth to the surface and contains a few mud lenses and is influenced from the nearby gravel road.

#### 4.7 Element distribution

The concentrations and the correlation of elements of Ca, Sr, Fe, Ti and K in MIL and C2L depend from the lithology (Table 4). Mean values for the elements in different sediment types of the cores are given in table 4. The element concentrations Fe, Ti, Ca Sr and K show positive correlations over the entire MIL core, which was computed by correlation matrices. Fe, Ti and K correlate positively with mud, whereas Sr correlates negatively with mud but positively with sand. The element concentrations oscillate strongly over the entire sediment core (Fig. 2).

For C2L, Ti and K show a positive correlation, which is stronger in blue-grey mud than in brown compacted mud. A moderate to strong negative correlation between Ca, Ti, K and Fe is evident in the blue-grey mud. In the peat layers in the deeper parts of C2L a negative correlation between Fe and Ti, K and also Sr is obvious, which is not observed in the brown compacted mud. (Fig. 3). Between 3.56 m and 4.4 m, the Ca values are high ( $\leq 65,000$  ppm), indicating a phase of higher marine influence. Sr is the only element, which correlates with grain size, in fact positively with sand and negatively with mud. Except for Ca, the concentration of all elements is higher and distribution curves are less oscillating than in the MIL sediment core.

#### 4.8 Grain size analysis

Grain size analysis of Mortagne 1L was undertaken only for the homogeneous dark-grey mud and laminated silty-sandy mud because of the likelihood of anthropogenic influence of the top layer of brown compacted mud. The averaged grain size is medium silt with varying percentages of clay and sand. All samples are very poorly sorted and fine skewed.

Brown compacted mud and blue-grey mud of CL2 are very poorly sorted and very fine skewed with mean values of 6.5–6.8 ( $\phi$ ). Values for the blue grey mud from StC are very similar, only differing with a mean value of 7.3 ( $\phi$ ). Sands from StC are poorly sorted, very coarse skewed

Table 4. Mean element concentrations of Mortagne 1L and Camp 2L for different lithologies.

Element Concentration in ppm	Homogeneous dark-grey mud	Laminated silty-sandy mud	Brown compacted mud		Blue-grey mud
	M1L	M1L	M1L	C2L	C2L
Ca	20,300	16,000	21,400	3,500	14,500
Sr	70	64	76.5	77	73
Fe	15,700	13,000	19,300	30,300	26,600
Ti	2,700	2,100	3,100	4,200	3,700
K	11,000	8,300	13,400	21,000	19,700

and have a mean of  $-0.55$  ( $\varphi$ ). Sand and gravel of Ozelle are very poorly sorted, coarse skewed and the mean value is  $0.4$  ( $\varphi$ ).

In the CM-diagram, all muds are situated in field VII and VIII, branch S-R and field T in terms of PASSEGA (1964, BRAVARD et al. 1986) and were transported as uniform (T) and uniform to graded suspension (S-R, Fig. 4B). Seven samples, six of them from the laminated silty-sandy layers of MIL, one from the blue grey mud of StCIL, plot separately in the upper Field VII above the S-R branch (Fig. 4A). For this a different facies or building process under higher energy conditions are likely. Sands and gravels from Ozelle and St. Ciers plot in field I and are transported depending from grain size by rolling and saltation (Q-P) and rolling (P-O-N) in a high-energy environment. Further interpretations are given in connection with the sediment types.

The bivariate plot of TANNER (1991) elaborated by LARIO et al. (2001) shows that all mud samples plot in the field of a filled estuary. The laminated silty-sandy mud plot at the transition to an open estuary indicating a higher energy level. Coarse grained samples do not plot in this diagram because of mean values  $\leq 1$ .

Minor differences between the sediments of the different locations themselves can be seen in the bivariate scattergram of skewness vs kurtosis (Fig. 4C). Muddy samples from StCiers and Mortagne have a skewness between c. 0.2 and 0.4, samples from Camp2 have a skewness around 1.0 but all are to classify as very fine skewed. In general coarser sediments plot slightly left of a symmetrical distribution (skewness  $+0.1$  to  $-0.1$ ), whereas muddy sediments, especially blue-grey mud, plot at the right side, but nearly all samples show a normal distribution (kurtosis 0.9–1.1).

## 5 Interpretation of the marsh infilling and environmental sequence

### 5.1 Sand and gravel

In the lower parts of Oz1, StCIL and StC1 sands and gravels occur in different compositions (Fig. 5). Sands from StCiers (branch Q-P, fields IV and I, Fig. 4B) are transported by rolling and saltation and sands and gravels from Ozelle (branch P-O-N, field I, Fig. 4B) are transported by rolling taking place in a fluvial regime as active channel fill and overbank deposits (FÜCHTBAUER & MÜLLER 1970, PEIRY 1988, BRAVARD & PEIRY 1999, MYCIELSKA-DOWIGIAŁŁO & LUDWIKOWSKA-KĘDZIA 2012). The gravel fraction encountered in the Oz1 core shows grain sizes above 20 mm interpreted as braided river sediments by JOUNNEAU et al. (1981). These sands and gravels are interpreted as belonging to the Pre Holocene (phase A, 15,000 BP –13,000 BP). Silty, clayey sands above (Oz1) show increasing mud content. This interval most likely marks the onset of estuarine infilling in the area near the valley slope. Sands and gravels of StC1 (branch Q to P, field I, Fig. 4B) are transported by saltation and rolling in a fluvial regime. They are interpreted as sediments of phase A too and sedimented in a greater distance from the valley slope.

### 5.2 Blue-Grey Mud

Blue-grey mud occurs in the cores from the southern and central part of the investigation area: C1–C3, StC1, StC2 and Br (Fig. 5). This medium plastic, homogenous mud reveals neither stratification nor any other sedimentary structures. A similar sediment is found in numerous other

salt marshes (e.g. ALLEN 2004, MORTIMER & RAE 2000, LARIO et al. 2001, GOODBRED et al. 1998) where it is often described as “green or grey-green mud”. In earlier studies of the St.-Ciers marsh (MELLALIEU et al. 2002) it was referred to as the “Lower Clay-Silt”.

The organic content is generally high, but varies according to depth and location. Samples show a high mica content, few poorly rounded quartz grains (< 250 µm), abundant fecal pellets and flocculated plant remains. Deposition took place by uniform and graded suspension under low energy conditions (Figs 4A, B) in an sheltered estuarine area (Fig. 4D), dead arms and areas which were temporary cut from the main stream (BRAVARD & PEIRY 1999). The high organic content and peat lenses indicate local stagnant water areas. Thicker peat accumulations may also be a consequence of stagnation of the sea level. Radiocarbon ages from the deepest part of C1 ( $7,971 \pm 44.5$  BP) and C3 ( $7,055 \pm 103.5$  BP) show that the sedimentation of blue-grey mud started before c 7,000 years BP in late Pleistocene to early Holocene (phase B) and ended diachronously, presumably depending on the existing morphology between around 6,500 BP and around 5,400 BP in the late Holocene (early phase C). Thickness is highest in C1 (> 11 m) near the recent main channel and decreases towards the east border of the valley where blue-grey mud is missing in Ozl. In the central part of the marsh around the Camp area, the mean sedimentation rate is estimated at 4 mm/y not concerning possible times of stagnation. Further northwest, between Beaumont and Camp the estuarine facies passes into a tidal mudflat facies (Fig. 5).

### 5.3 Dark grey mud and laminated silty-sandy mud

Dark-grey, homogeneous mud and laminated silty-sandy mud are only found in the northern study area in the Mortagne and Beaufort boreholes (Fig. 5). The most frequent foraminifera of MIL are *Haynesina germanica*, *Ammonia tepida*, and *Trochammina inflata* (table 3) which indicate intertidal mudflats and estuarine milieus (HOFKER 1977, DEBENAY et al. 2000, FIORINI 2004, DUCHEMIN et al. 2005, HORTON & EDWARDS 2006, MURRAY 2006, DUPUY et al. 2010, KOHO & PIÑA-OCHOA 2012). The bivalve *Scrobicularia*, endobenthos of the muddy intervals, lives also in intertidal mud flats and estuaries (SANTOS et al. 2011, PIZZOLA 2002). A marine influence is documented by abundant spines of sea urchins, sponge spicules, a small amount of benthic foraminifera from open sea, shelf and normal marine environments (Table 3). The dark-grey mud is settled by uniform suspension (branch S-R, field VIII, VII, Fig. 4B) in a restricted estuarine regime (Fig. 4D) whereas the sedimentation of the laminated silty-sandy mud took place by uniform to graded suspension (branch S-R, field VII, Fig. 4B) in an estuarine realm (Fig. 4D). The difference between mud and laminated silt is due to changing water energy in a tidal regime for example around shifting tidal channels or during storms what can be recognized from the intercalation of fine silty planar, oblique or undulated laminae. The facies of Mortagne and Beaufort boreholes can be described as a tidal mudflat with tidal channels of changing spread developed during phase B. The alternating of mud and laminated silt layers may also reflect the temporary stagnation in relative sea level rise as assumed by JOUANNEAU & LATOUCHE (1981).

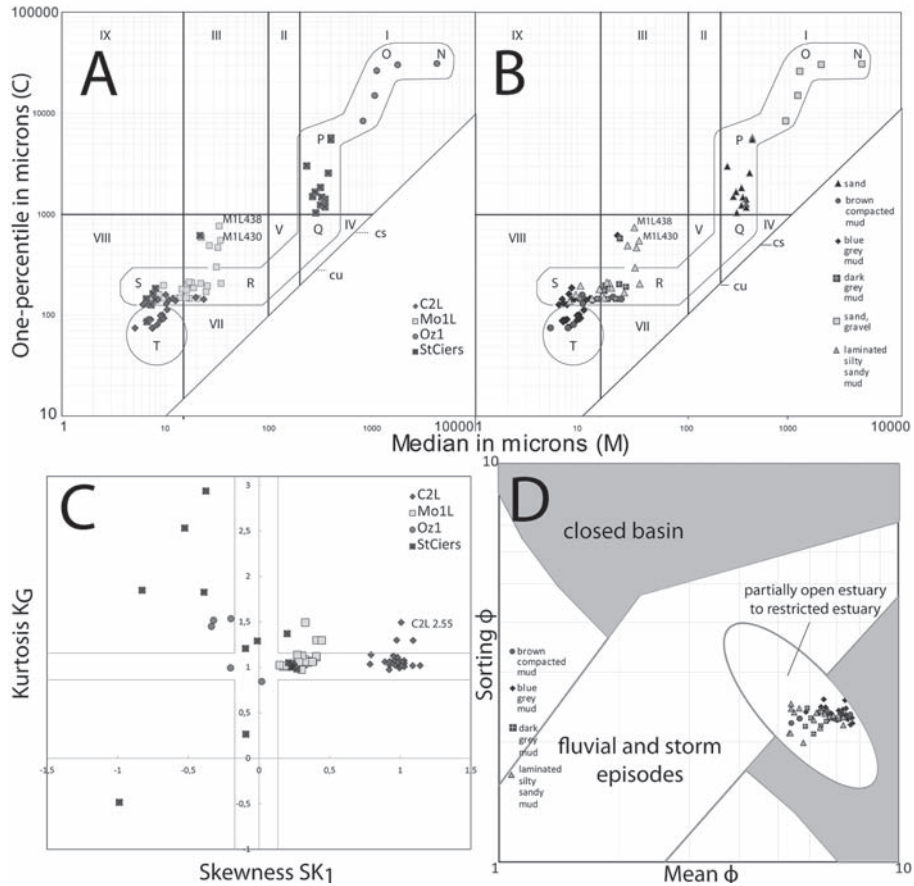
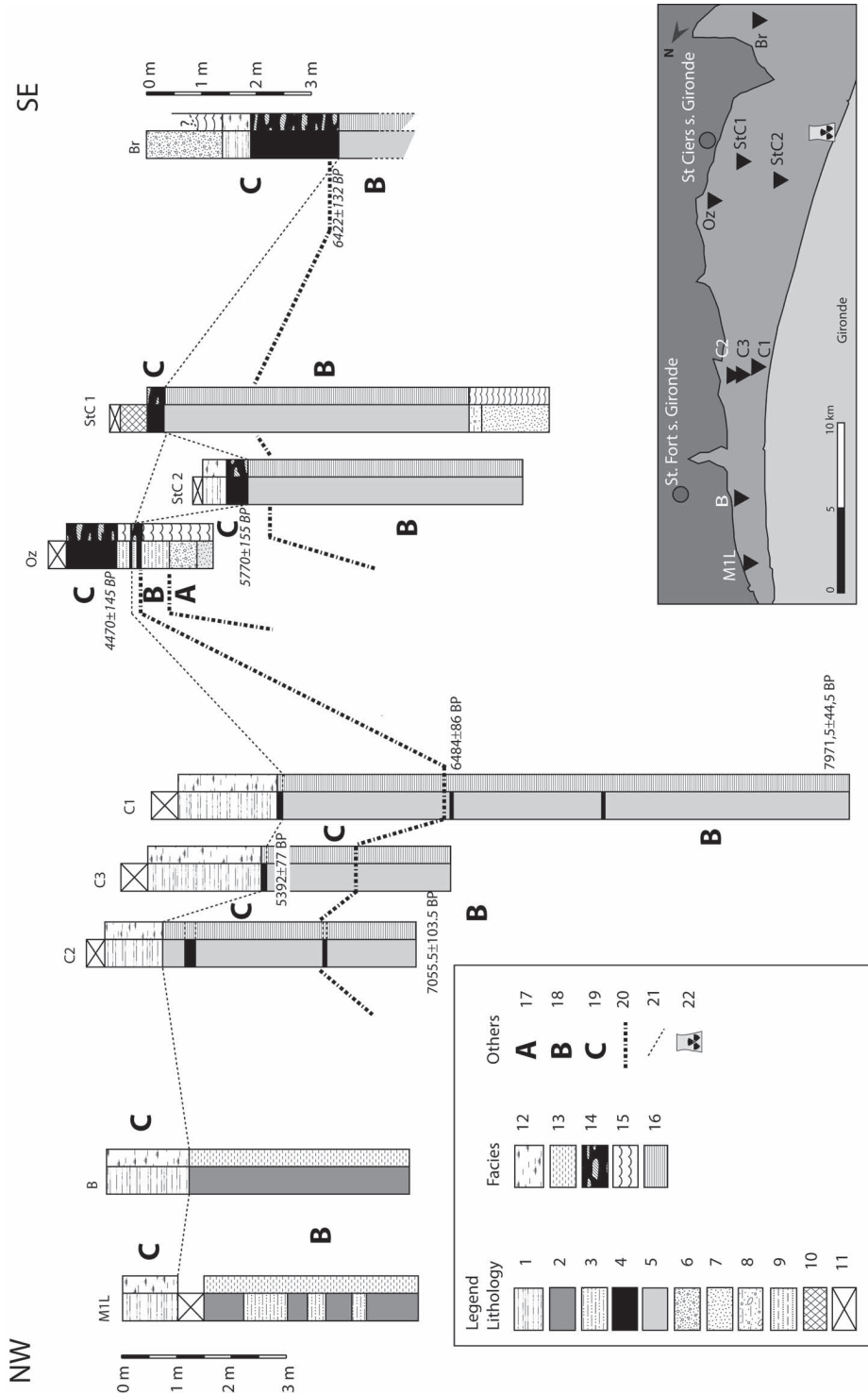


Fig. 4. CM-diagrams (after PASSEGA 1964, PASSEGA & BYRAMJEE 1969, elaborated by MYCIELSKA-DOWGIALŁO & LUDWIKOWSKA-KĘDZIA (2011)), cu: upper limit of uniform suspension, cs: upper limit of graded suspension. Transport mechanism: O–N–P: rolling, P–Q: rolling and saltation, Q–R: graded suspension, S–R: graded and uniform suspension, T: uniform suspension. A: Plot sorted by location, B: Plot sorted by sediment type. C: Bivariate scattergram skewness vs kurtosis sorted by location, D: Bivariate scattergram of TANNER (1991) elaborated by LARIO et al. (2001), samples sorted by sediment type.

Fig. 5. Schematic cross section through the drilling area from NW to SE of the St Ciers-sur-Gironde marsh showing the evolution of the marsh from the Holocene transgression to recent. ►

Legend: Lithology: 1 – brown compacted mud, 2 – homogeneous dark grey mud, 3 – laminated silty-sandy mud, 4 – peat and organic rich mud, 5 – blue-grey mud, 6 – gravel, 7 – fine sand, 8 coarse sand with gravel and clay, 9 – clayey, silty sand, 10 – embankment, 11 – core loss, caving material; Facies: 12 – marsh, 13 – tidal mudflat, partly with tidal channels, 14 – stagnant water, floodplain, 15 – fluvial facies, 16 – estuarine milieu; Others: 17 – A – Pre-Holocene, 18 – B – Late Pleistocene to early Holocene, 19 – C: Late Holocene to present, 20 – timelines between the phases of evolution, 21 – facies boundary, 22 – Blayais power plant. Ages in *italic letters* are from MELLALIEUX et al. (2000). Dates are from the base of upper peat layers from the nearby drillings HOREST 9607, HOREST 9608 and HOREST 9611/12.



#### 5.4 *Peat and black organic rich mud*

The black, organic, rich mud and peat are closely linked to each other, with sometimes the mud, sometimes the peat constituting the main part. The sedimentation process of the black organic rich mud is similar to that of the brown compacted mud (Fig. 4B). Thick peat layers occur at Oz1, StC2 at the base of brown compacted mud, in Br and in StC1 below anthropogenic material. Peat units sometimes show sharp contacts to the underlying blue grey mud. The layers are thicker in the southeastern marsh area and thin out towards the northwestern but they can be correlated laterally between Br, StC1, StC2, Oz1, C1 and C2 (Fig. 5). The StCiers cores were drilled in an area that was under water until Roman times, but with a limited connection to the main river, which provided good conditions for peat formation. (MELLALIEUX et al. 2000, COQUILLAS, 2004). In the Camp and St.-Ciers areas the peat layers are younger than 6,000 years BP and were built during the Late Holocene (Phase C), while in the Southeast (Br) they are slightly older and therefore their basal parts still belong in Phase B. Peat and black organic rich mud are built in areas with stagnant water, abandoned channels and on the floodplain. Ages of several peat layers across the St. Ciers marsh from MELLALIEU et al. (2000) range from  $2,802 \pm 77.5$  BP to  $6,422.5 \pm 132.5$  BP and confirm that major peat building started at the end of phase B and in lower phase C. Single well defined thin peat layers also occur within blue grey mud in C2 and C2L. Radiocarbon dating of the peat from C1 (5.42 m – 5.51 m, NUG-2) gives an age of  $6,484 \pm 86$  BP (table 2), so it was built in phase B as is supposed for all peat layers within blue-grey mud of C1 and C3.

#### 5.5 *Brown Compacted Mud*

The uppermost layer of the marsh is built of the brown compacted mud and is found in M1L, B, C1 to C3 and StC2 sediment cores (Fig. 5), where it was not replaced by anthropogenic re-fill. Carbonate concretions, as they also occur in today's drainage ditches near the outcrops of Cretaceous limestones, appear at different depths. They have probably formed in phases of a constant groundwater level. Brown compacted mud can be interpreted as sediment settled of uniform suspension (lower branch S-R field T, Fig. 4,B) in swampy areas. In comparison with other fluvial and estuarine regimes (BRAVARD et al. 1986, PEIRY 1988, BRAVARD & PEIRY 1999, MYCIELSKA-DOWIGIAŁŁO & LUDWIKOWSKA-KĘDZIA 2012) and taking in account the TANNER (1991) diagram (Fig. 4,D) the environment can be interpreted as floodplain and in parts as stagnant water regime. Peat at the base of the brown compacted mud in cores from the Camp area is built in stagnant water areas like lakes and on the marsh plain. As youngest layer of the marsh, the brown compacted mud is substantially influenced by human activity in its upper parts. Radiocarbon dating from the peat at the base of the brown compacted mud give ages of  $5,392 \pm 77$  BP (C3, NUG-4) and after MELLALIEU et al. (2000)  $4,470 \pm 155$  BP (HO 99608) and  $5,770 \pm 155$  BP (HO 99607) (table 2). So the whole sequence is built during the Late Holocene until the present in phase C (Fig. 5). With reference to ALLEN & POSAMENTIER (1993) and JOUANNEAU & LATOUCHE (1981), sediments of M1L are as well interpreted to be of late Holocene age. The presence of relatively thick, brown compacted mud especially in the Camp area points to a much slower sea level rise (KIDSON 1982, FAIRBRIDGE 1961) or maybe phases of equilibrium (DYER 1998).

## 5.6 Summary

Over wide parts of the marsh the cores show a set of similar lithologies above the Eocene substratum and the basal Holocene. From bottom to top, the sequence reflects the evolution of a filling estuary with decreasing tidal influence on a marshland and also the evolution from a fluvial high-energy environment to the low-energy environment of the estuary and the marshland. In the tidal area, only fine-grained sediments are deposited, although the tides are expected to produce higher water energies. Each type of sediment reflects conditions that are considered stable for the time of the deposition. They represent the background in which storms, at best, leave detectable patterns.

## 6 Discussion on potential evidence for palaeostorm deposits

Various characteristics of storm events in tidal and marsh areas are looked for: Storm deposits in an estuarine mudflat should start with a thinning-up sequence of sandy laminae upon an erosional base wherein shell debris, mud clasts and typical faunal assemblages from the subtidal zone occur (YANG et al. 2007, HIPPENSTEEL & MARTIN 2009). GOODBRED & HINE (1995) determined that storm sediments in marsh areas are composed of coarse silts with few organics. ALLEN (1991) mentioned the “rip-off” of millimeter to decimeter sized peat and strew lumps from adjacent cliffs after a storm. Grain size analyses also show good results in the detection of storm sediments (LARIO et al. 2001). After the flooding caused by the extratropical cyclon, “Lothar” and “Martin”, SALOMON (2002) observed the deposition of a 15 cm thick mud layer on the surface of the St.-Ciers marsh, a characteristic that can serve here as an additional indicator. The element concentrations, the available sediments and their depositional environment were also taken into account.

### 6.1 Homogeneous blue-grey mud – sheltered estuarine facies

The blue-green mud is very homogeneous and has no sediment structures that could indicate storm deposits. In C1 abundant plant debris and peat lenses, that could correspond to peat and strew lumps as described for storms by ALLEN (1991), could neither be related to grain size distribution, Ca and Sr element distribution nor could they be related to similar horizons in boreholes over the marsh. Sr, the only element that correlates positively with sand of possibly marine origin (ALLEN 1991), has two distinct peaks (C2L, Fig. 3), while Ti and K concentrations decrease. This may be due to a short-term higher marine influence, possibly a storm event, but cannot be confirmed by other characteristics. The lack of more significant evidence may indicate that during the deposition of the blue-grey mud the most of the area was outside the effects of storm events.

### 6.2 Dark grey mud and laminated silty-sandy mud – tidal mudflat facies

In MIL, between 4.26 m – 4.38 m two thinning upward successions (4.26 m – 4.30 m, 4.32 m – 4.38 m, Fig. 2) occur wherein element distributions correlates well with grain size. But there is no erosion or erosional contact like described by SHI & CHEN (1996) and ALLEN (2004) for storm deposits. On the other side, the marine influence indicated by Ca and Sr concentrations in-

creases while Fe, Ti and K values as terrestrial indicators decrease and sedimentation took place under slightly higher energy (Fig. 4A, 4B, MIL438, MIL430). Another reasonable hypothesis is that the observed succession results from a depositional environment in close proximity to a tidal channel overflowing under storm conditions and / or spring tides. If phases of high-energy deposition are related to enhanced entry of material from the estuary mouth, this may be the reason for the decrease of Fe, Ti and K concentrations and the increase of Ca and Sr concentrations. The MIL core shows repeatedly deposits of thin, silty, planar, oblique or wavy lamellae in the dark-grey mud and in the laminated silty-sandy mud, which can be interpreted both as result of storm events and as sediment structures of tidal flats. In 6 of 13 samples of core MIL a small amount of the genera *Bolivina*, *Bulimina* and *Lagena* in both laminated silty-sandy mud and homogeneous dark-grey mud are found (Table 3). In intertidal areas of the British Isles it has been observed that they are transported under energy-rich conditions into estuaries and marshes. (HORTON & EDWARDS 2006). Magnetic susceptibility and element concentrations show no apparent correlations between samples with and without these foraminifera with the exception of MIL 512–521 and MIL 336–343 (Fig. 3). Because the samples were taken over a 5–8 cm long section, they sometimes comprise several laminae and the resolution is therefore coarser than that of the XRF, also the number of individuals is too small for a quantitative analysis. High resolution scanning and  $\mu$ -XRF can help to distinguish whether the laminae originate from tidal processes or from storm activity.

### 6.3 *Brown compacted mud – marsh facies*

The occurrence of barchan dunes at the Atlantic coast from 2,000 BP to the 18<sup>th</sup> century may be due to an increase in storm activity (PONTEE et al. 1998) that may have left traces on the marsh surface. Pure mud layers similar to the deposits of the cyclon “Lothar” und “Martin” do not show up in the boreholes. However, some Bolivinoids and Buliminoids in C2 and also in C2L together with slightly differing skewness and kurtosis at the depth of 2.55 m (Fig. 4C, C2L 2.55) as well as some coarse silt and fine sand laminae and lenses which contain well rounded quartz grains may indicate temporarily changed deposition conditions.

### 6.4 *Summary*

On the St. Ciers-sur-Gironde march the conditions for the preservation of distinct storm layers are limited. The Wadden Sea in the northwestern part of the swamp has the best conservation potential. Sediments deposited by storms and floods are mainly of fluvial origin and therefore a change in grain size is not always discernible. The magnetic susceptibility together with its positive correlation with Fe and Ti and its negative correlation with Ca and Sr indicate short-term changes in the sedimentation process. However, we assume that the magnetic susceptibility and chemistry of sediments are in many cases quickly overshadowed by the influence of tidal regime and fluvial input. Layers of previous high-energy events on the surface of the salt marsh may have been erased during pedogenesis. In addition, storm deposits can be eroded during the mid-ebb and mid-flood, when the erosion in the estuary is strongest (ROBERT et al. 2004).

Furthermore, more emphasis should be placed on the uppermost metre of the core to identify more recent storm deposits. The analysis of grain size in further studies may take into account the removal of carbonates during sample preparation.

## 7 Conclusion

- The results of the drill profiles, grain size analyses, geochemical and geophysical as well as micropaleontological investigations confirm and complement the late Pleistocene to Holocene development of the marsh described from previous studies. A profile from NW to SE (Fig. 5) illustrates evolution and distribution of facies from a fluvial regime to an estuarine environment and at least to a salt marsh on the eastern bank of the Gironde valley
- During the pre-Holocene (phase A: 15,000 BP – 13,000 BP) in the young Gironde valley a high-energy fluvial regime with active channels and overbank deposits was established in which mainly sand and gravel were deposited. After JOUANNEAU & LATOUCHE (1981) it was a braided river system in the beginning. Sediments of phase A are drilled near the old valley slope near St. Ciers-sur-Gironde.
- Two different facies occur from the Late Pleistocene to early Holocene (phase B: 13,000 BP – 6,000 BP). In the southeastern and central part of the valley blue-grey mud and locally peat were deposited under low energy conditions in a sheltered estuarine area, dead arms and areas which were temporary cut from the main stream. Thickness is highest in the Camp area where a mean sedimentation rate of 4 mm/y is estimated. Deposition of blue-grey mud started before c.  $7,971.5 \pm 44.5$  BP. Two distinct peat layers may show sea level stagnation. To the northwest this estuarine facies changes to a tidal mudflat with shifting channels of different extent. Typical sediments are dark-grey mud and laminated silty-sandy mud.
- The last stage is the formation of the salt marsh over the whole investigation area in the Late Holocene to present (phase C: 6,000 BP- present). Characteristically, this phase begins with peat and black organic rich mud but radiocarbon ages show that the base of the peats is diachronous from the Southeast to the Northwest. Near Braud-et-St.-Louis, the facies change is dated back to the highest part of phase C.
- The main sediment load, also during storm events such as “Lothar” and “Martin”, comes from the Garonne and Dordogne rivers, so that a marine signature in form of chemical elements (Ca, Sr vs. Fe, Ti, K), microfossils and grain size is only weakly expressed in the brown compacted mud. A number of factors influence deposition and preservation of storm events like anthropogenic and natural processes which overprint the effects of flooding and storm events considerably on the marsh surface so that no clear traces of palaeostorms have been detected. However, evidence of storm deposits was found in the tidal mudflats in the northern part of the study area near Mortagne-sur-Gironde. The southward adjacent part of the estuary where blue-grey mud has been deposited may be mostly out of reach of storm events.

### Acknowledgements

We would like to thank the drilling team Malte Rebentisch, Julian Geers, Matthias Kunz, Daniel Kayser, Tabea Schröder and Joska Röth for their efforts during fieldwork and in the laboratory. Special thanks to the team of the laboratory of Physical Geography at the RWTH Aachen for conducting the laser-granulometry. Finally we would like to thank the inhabitants of the area who gave us informations about the history of the places and the permission to drill at their sites.

## References

- AGENCE DE L'EAU ADOUR GARONNE (ed) (1994): Synthèse des Connaissances de l'Estuaire de la Gironde. – 289 pp; online available: [archimer.ifremer.fr/doc/00106/21708/19287.pdf](http://archimer.ifremer.fr/doc/00106/21708/19287.pdf)
- ALAVI, S. N. (1988): Late Holocene Deep-Sea Benthic Foraminifera from the Sea of Marmara. – *Marine Micropaleontology* **13** (1988): 213–237.
- ALLEN, G. P. (1973): Étude des processus sédimentaires dans l'estuaire de la Gironde. – *Mémoires de l'Institut de géologie du bassin d'Aquitaine* **5**: 314 pp.
- ALLEN, G. P. (1991): Sedimentary Processes and Facies in the Gironde Estuary: A Recent Model for Macrotidal Estuarine Systems. CSPG Special Publications. – *Clastic Tidal Sedimentology Memoir* **16**: 29–39.
- ALLEN, G. P., CASTAIGN, P., FROIDEFOIS, J. M. & MIGNIOT, C. (1979): Quelques effets à long terme des aménagements sur la sédimentation dans l'estuaire de la Gironde. – *Les côtes atlantiques d'Europe, évolution, aménagement, protection* **15–16** (9): 115–138.
- ALLEN, G. P. & POSAMENTIER, H. W. (1993): Sequence stratigraphy and facies model of an incised valley fill the Gironde Estuary, France. – *Journal of sedimentary petrology* **63** (3): 378–391.
- ALLEN, J. R. L. (2000): Morphodynamics of Holocene salt marshes: a review sketch from the Atlantic and Southern North Sea coasts of Europe. – *Quaternary Science Reviews* **19** (12): 1155–1231.
- ALLEN, J. R. L. (2004): Annual textural banding in Holocene estuarine silts, Severn Estuary Levels (SW Britain): patterns, cause and implications. – *The Holocene* **14** (4): 536–552.
- BILLY, J., CHAUMILLON, E., FÉNIÈS, H. & POIRIER, C. (2012): Tidal and fluvial controls on the morphological evolution of a lobate estuarine tidal bar: The Plassac Tidal Bar in the Gironde Estuary (France). – *Geomorphology* **169–170**: 86–97.
- BITEAU, J. J., LE MARREC, A., LE VOT, M. & MASSET, J. M. (2006): The Aquitaine Basin. – *Petroleum Geoscience* **12**: 247–273.
- BRAVARD, J. P., AMOROS, C. & JACQUET, G. (1986): Reconstitution de l'environnement des sites archéologiques fluviaux par une méthode interdisciplinaire associant la géomorphologie, la zoologie et l'écologie. – *Revue d'Archéométrie* **10** (1986): 43–55.
- BRAVARD, J. P., GOICHOT, M. & TRONCHÈRE, H. (2014): An assessment of sediment-transport processes in the Lower Mekong River based on deposit grain sizes, the CM technique and flow-energy data. – *Geomorphology* **207**: 174–189.
- BRAVARD, J. P. & PEIRY, J. L. (1999): The CM pattern as a tool for the classification of alluvial suites and floodplains along the river continuum. – *Geological Society, London, Special Publications* **163**: 259–268; <https://doi.org/10.1144/GSL.SP.1999.163.01.20>.
- BRONK RAMSEY, C. (2009): Bayesian analysis of radiocarbon dates. – *Radiocarbon* **51** (1): 337–360.
- CASTAIGN, P. & ALLEN, G. P. (1981): Mechanisms controlling seaward escape of suspended sediment from the Gironde. A macrotidal estuary in France. – *Marine Geology* **40** (1–2): 101–118; doi: 10.1016/0025-3227(81)90045-1.
- COQUILLAS, D. (2004): Approche diachronique et évolution des marais de la rive droite de la Gironde. – *æstuarina* **5**: 145–170.
- DALRYMPLE, R. W., ZAITLIN, B. A. & BOYD, R. (1992): Estuarine facies models: conceptual basis and stratigraphic implications. – *Sedimentary Geology* **62** (6): 1130–1146.
- DEARING, J. (1999): Environmental Magnetic Susceptibility. – Using the Bartington MS2 System. – 54 pp.
- DEBENAY, J.-P. & GUILLOU, J.-J. (2002): Ecological transitions indicated by foraminiferal assemblages in paralic environments. – *Estuaries* **25** (6A): 1107–1120.
- DEBENAY, J.-P., GUILLOU, J.-J., REDOIS, F. & GESLIN, E. (2000): Distribution trends of foraminiferal assemblages in paralic environments. A base for foraminifera as bioindicators. – In: MARTIN, R. E. (ed.): *Environmental Micropaleontology: The Application of Microfossils to Environmental Geology*. – *Topics in Geobiology* **15**: 39–67.
- DICKSON, A. G. & GOYET, C. (ed.) (1994): Handbook of methods for the analysis of the various parameters of the carbon dioxide system in sea water. – 2<sup>nd</sup> edition, ORNL/CDIAC-74; <https://www.nodc.noaa.gov/ocads/oceans/handbook.html> [14.04.2018].
- DIN 18123:1996-11 (1996): Baugrund, Untersuchung von Bodenproben – Bestimmung der Korngrößenverteilung. – Beuth, Berlin, 12 pp.

- DOUBREUILH, J., CAPOEUILLE, J.-P., FARJANEL, G., KARNAY, G., PLATEL, J. P. & SIMON-COINÇON, R. (1995): Dynamique d'un comblement continental néogène et quaternaire: l'exemple du bassin d'Aquitaine. – *Geologie de la France* **4**: 3–26.
- DUCHEMIN, G., JORISSEN, F. J., REDOIS, F. & DEBENAY, J. P. (2005): Foraminiferal microhabitats in a high marsh: Consequences for reconstructing past sea levels. – *Palaeogeography, Palaeoclimatology, Palaeoecology* **226** (1–2): 167–185.
- DUPUY, CH., ROSSIGNOL, L., GESLIN, E. & PASCAL, P.-Y. (2010): Predation of mudflat meio-macrofaunal metazoans by a calcareous foraminifer, *Ammonia tepida* (Cushman, 1926). – *Journal of Foraminiferal Research* **4** (4): 305–312.
- DYER, K. R. (1998): The typology of intertidal mudflats. – Geological Society, London, Special Publications **139** (1): 11–24.
- FAIRBRIDGE, R. W. (1961): Eustatic changes in sea level. – *Physics and Chemistry of the Earth* **4**: 99–185.
- FENIES, H. & TASTET, J.-P. (1998): Facies and architecture of an estuarine tidal bar (the Trompeloup bar, Gironde Estuary, SW France). – *Marine Geology* **150** (1–4): 149–169.
- FIORINI, F. (2004): Benthic foraminiferal associations from Upper Quaternary deposits of southeastern Po Plain, Italy. – *Micropaleontology* **50** (1): 45–58.
- FOLK, R. L. & WARD, W. C. (1957): Brazos River bar: a study in the significance of grain size parameters. – *Journal of Sedimentary Petrology* **27**: 3–26.
- FÜCHTBAUER, H. & MÜLLER, G. (1970): *Sediment-Petrologie. Teil II Sedimente und Sedimentgesteine.* – Schweizerbart Science Publishers, Stuttgart, 1142 pp.
- GHAIN, D., NZIOKA MUTUA, A. & TAN, L. (2014): Sediment and hydrodynamic profile of the Gironde estuary, France. – Technical Report, 20 pp.
- GORBATCHEV, A., MATTÉI, J. M., REBOUR, V. & VIAL, E. (2001): Report on flooding of Le Blayais power plant on 27 December 1999. – Gesellschaft für Anlagen- und Reaktorsicherheit mbH (GRS), Koeln (Germany); [vp.]:15 pp; EUROSAFE 2000: International forum for nuclear safety; 6.–7. Nov. 2000.
- GOODBRED, S. L. J. & HINE, A. C. (1995): Coastal storm deposition: Salt-marsh response to a severe extratropical storm, March 1993, west-central Florida. – *Geology* **23** (8): 679–682.
- GOODBRED, S. L. J., WRIGHT, E. E. & HINE, A. C. (1998): Sea-Level Change and Storm-Surge Deposition in a Late Holocene Florida Salt Marsh. – *Journal of Sedimentary Research* **68** (2): 240–252.
- GRANBOULAN, J., FERAL, A. & VILLEROT, M. (1989): Study of the Sedimentological and Rheological Properties of Fluid Mud in the Fluvio-estuarine System of the Gironde Estuary. – *Ocean & Shoreline Management* **12** (1989): 23–46.
- HARFF, J., FLEMMING, N. C., GROH, A., HÜNICKE, B., LERICOLAIS, G., MESCHEDÉ, M., ROSENTAU, A., SAKEL-LARIOU, D., USCINOWICZ, S., ZHANG, W. & ZORITA, E. (2017): Sea Level and Climate. – In: FLEMMING, N. C., HARFF, J., MOURA, D., BURGESS, A. & BAILEY, G. N. (eds): *Submerged Landscapes of the European Continental Shelf. – Quaternary Paleoenvironments*, Wiley, Blackwell, 11–49.
- HAYWARD, B. W., GRENFELL, H. R., SABAA, A. T., CARTER, R., COCHRAN, U., LIPPS, J. H., SHANE, PH. R. & MORLEY, M. S. (2006): Micropaleontological evidence of large earthquakes in the past 7200 years in southern Hawke's Bay, New Zealand. – *Quaternary Science Reviews* **25** (11–12): 1186–1207.
- HAYWARD, B. W., GRENFELL, H. R., SABAA, A. T., NEIL, H. & BUZAS, M. A. (2010): Recent New Zealand deep-water benthic foraminifera: Taxonomy, ecologic distribution, biogeography, and use in paleoenvironmental assessment. – *GNS Science Monograph* **26**: 363 pp.
- HIPPENSTEEL, S. P. & MARTIN, R. E. (1999). Foraminifera as an indicator of over-wash deposits, Barrier Island sediment supply, and Barrier Island evolution: Folly Island, South Carolina. – *Palaeogeography, Palaeoclimatology, Palaeoecology* **149** (1–4): 115–125.
- HOFKER, J. (1977): The foraminifera of dutch tidal flats and salt marshes. – *Netherlands Journal of Sea Research* **11** (3–4): 223–296.
- HOLBOURN, A., HENDERSON, A. S. & MACLEOD, N. (2013): *Atlas of Benthic Foraminifera*. First edition. – Wiley, 642 pp.
- HORTON, B. P. & EDWARDS, R. J. (2006): Quantifying Holocene sea-level change using intertidal foraminifera: lessons from the British Isles. – *Cushman Foundation Special Publication* **40**: 1–97.
- HORTON, B. P. & MURRAY, J. W. (2007): The roles of elevation and salinity as primary controls on living foraminiferal distributions: Cowpen Marsh, Tees Estuary, UK. – *Marine Micropaleontology* **63**: 169–186.

- JOUANNEAU, J.-M. (1973): Bilan des connaissances sur la rive droite de la Gironde. – Centre National pour l'exploitation des océans, Institut de Géologie du bassin d'Aquitaine, Talence. 26 pp; <http://archimer.ifremer.fr/doc/00080/19155/16755.pdf>.
- JOUANNEAU, J.-M. & LATOUCHE, C. (1981): The Gironde estuary. – *Contributions to Sedimentology* **10**: 115 pp.
- KAPSIMALIS, V., MASSÉ, L., VELEGRAKIS, A., TASTET, J., LAGASQUIE, M. & PAIREAU, O. (2004): Formation and growth of an estuarine sandbank: Saint-Georges Bank, Gironde Estuary (France). – *Journal of Coastal Research* **SI 41**: 27–42.
- KIDSON, C. (1982): Sea level changes in the holocene. – *Quaternary Science Reviews* **1** (2): 121–151.
- KOHO, K. A. & PIÑA-OCHOA, E. (2012): Benthic Foraminifera: Inhabitants of Low-Oxygen Environments. – In: ALTENBACH, A. V., BERNHARD, J. M. & SECKBACH, J. (eds): *Anoxia Evidence for Eukaryote Survival and Paleontological Strategies*, 249–285.
- LAMBECK, K. (1997): Sea-level change along the French Atlantic and Channel coasts since the time of the Last Glacial Maximum. – *Palaeogeography, Palaeoclimatology, Palaeoecology* **129** (1–2): 1–22.
- LAMBECK, K., ROUBY, H., PURCELL, A., SUN, Y. & SAMBRIDGE, M. (2014): Sea level and ice volume since the glacial maximum. – *Proceedings of the National Academy of Sciences* **111** (43): 15296–15303; doi: 10.1073/pnas.1411762111.
- LARIO, J., ZAZO, C., PLATER, A. J., GOY, J. L., DABRIO, C. J., BOJA, F. & LUQUE, L. (2001): Particle size and magnetic properties of Holocene estuarine deposits from the Donana National Park (SW Iberia): evidence of gradual and abrupt coastal sedimentation. – *Zeitschrift für Geomorphologie NF* **45** (1): 33–54.
- LARROSE, A., COYNEL, A., SCHÄFER, J., BLANC, G., MASSÉ, L. & MANEUX, E. (2010): Assessing the current state of the Gironde Estuary by mapping priority contaminant distribution and risk potential in surface sediment. – *Applied Geochemistry* **25** (12): 1912–1923.
- LESUEUR, P., TASTET, J. P. & WEBER, O. (2002): Origin and morphosedimentary evolution of fine-grained modern continental shelf deposits. The Gironde mud fields (Bay of Biscay, France). – *Sedimentology* **49** (6): 1299–1320; doi: 10.1046/j.1365-3091.2002.00498.x.
- MELLALIEU, S. J., MASSÉ, L., COQUILLAS, D., ALFONSO, S. & TASTET, J.-P. (2000): Holocene development of the east bank of the Gironde Estuary: geoarchaeological investigation of the Saint Ciers-sur-Gironde marsh. – In: PYE, K. & J ALLEN, R. L. (eds): *Coastal and Estuarine Environments: sedimentology, geomorphology and geoarchaeology*. – *Geological Society of London* **175**: 317–341.
- MIGNIOT, C. (1971): Évolution de la Gironde au cours des temps. – *Bulletin de l'Institut de Géologie du Bassin d'Aquitaine* **2** (11): 221–279.
- MORTIMER, R. J. G. & RAE, J. E. (2000): Metal Speciation (Cu, Zn, Pb, Cd) and Organic Matter in Oxidic to Suboxic Salt Marsh Sediments, Severn Estuary, Southwest Britain. – *Marine Pollution Bulletin* **40** (5): 377–386.
- MUIR, M. A. K. (2013): Gironde Estuary. – *Biomes & Ecosystems* **2**: 594–596; [http://www.eucc.net/en/climate\\_change/MAKMuir-GirondeEstuaryArticle.pdf](http://www.eucc.net/en/climate_change/MAKMuir-GirondeEstuaryArticle.pdf) [06.02.2015]
- MURRAY, J. W. (2006): *Ecology and Applications of Benthic Foraminifera*. – Cambridge University Press, Cambridge, 426 pp.
- MYCIELSKA-DOWGIAŁO, E. & LUDWIKOWSKA-KĘDZIA, M. (2012): Alternative interpretations of grain-size data from Quaternary deposits. – *Geologos* **17** (4): 189–203; doi: 10.2478/v10118-011-0010-9.
- PASSEGA, R. (1957): Texture as Characteristic of Clastic Deposition. – *AAPG Bulletin* **41**: 1952–1984.
- PASSEGA, R. (1964): Grain size representation by CM patterns as a geologic tool. – *Journal of Sedimentary Research* **34** (4): 830–847.
- PASSEGA, R. & BYRAMJEE, R. (1969): Grain-size image of clastic deposits. – *Sedimentology* **13** (3–4): 233–252.
- PEIRY, J.-L. (1988): *Approche géographique de la dynamique spatio-temporelle des sédiments d'un cours d'eau intra-montagnard: l'exemple de la plaine alluviale de l'Arve Haute-Savoie*. PhD, 3. University Jean-Moulin Lyon, France.
- PIZZOLLA, P. F. (2002): *Scrobicularia plana* – Peppery furrow shell. – In: TYLER-WALTERS, H. & HISCOCK K. (eds): *Marine Life Information Network: Biology and Sensitivity Key Information Reviews* [online]. Plymouth: Marine Biological Association of the United Kingdom. <https://www.marlin.ac.uk/species/detail/1507>, [cited 26-04-2018].

- PLATEL, J. P. (1987): Le Crétacé supérieur de la plate-forme septentrionale du bassin d'Aquitaine. Stratigraphie et évolution géodynamique. Thèse Doctorat d'Etat ès-Sciences, Université de Bordeaux III. – Documents BRGM **164** (1989): 573 pp.
- PONTEE, N. I., TASTET, J.-P. & MASSE, L. (1998): Morpho-sedimentary evidence of Holocene coastal changes near the mouth of the Gironde and on the Medoc Peninsula, SW France. – *Oceanologica Acta*: **21** (2): 243–261.
- PRITCHARD, D. W. (1967): What is an estuary: Physical Viewpoint. – American Association for the Advancement of Science Publication **83**: 3–5.
- REIMER, P. J., BARD, E., BAYLISS, A., BECK, J. W., BLACKWELL, P. G., BRONK RAMSEY, C., GROOTES, P. M., GUILDERSON, T. P., HAFLIDASON, H., HAJDAS, I., HATTŽ, C., HEATON, T. J., HOFFMANN, D. L., HOGG, A. G., HUGHEN, K. A., KAISER, K. F., KROMER, B., MANNING, S. W., NIU, M., REIMER, R. W., RICHARDS, D. A., SCOTT, E. M., SOUTHON, J. R., STAFF, R. A., TURNEY, C. S. M. & VAN DER PLICHT, J. (2013): IntCal13 and Marine13 Radiocarbon Age Calibration Curves 0–50,000 Years cal BP. – *Radiocarbon* **55** (4): 1869–1887.
- RISKNAT.ORG (ed) (2001): Palaeo-environmental Study Area P16. East Bank of the Gironde Area, West Coast, France. – in collaboration with TASTET, J. P. (Rapport Activité Ateliers), [http://www.risknat.org/projets/riskydrogeo/docs/guide\\_pratique/Acivite1\\_Ateliers/Presentations%20Atelier1/A1P13-Coastal%20changes/vol2/p16.pdf](http://www.risknat.org/projets/riskydrogeo/docs/guide_pratique/Acivite1_Ateliers/Presentations%20Atelier1/A1P13-Coastal%20changes/vol2/p16.pdf); [09.02.2015].
- ROBERT, S., BLANC, G., SCHÄFER, J., LAVAUX, G. & ABRIL, G. (2004): Metal mobilization in the Gironde Estuary (France): the role of the soft mud layer in the maximum turbidity zone. – *Marine Chemistry* **87** (1–2): 1–13.
- SAGEMAN, B. B. & LYONS, W. (2003): Geochemistry of Fine-grained Sediments and Sedimentary Rocks. – In: HOLLAND, H. D. & TUREKIAN, K. K. (eds): *Treatise in Geochemistry* **7**: 115–158, Elsevier Science.
- SALOMON, J.-N. (2002): Linondation dans la basse vallée de la Garonne et l'estuaire de la Gironde lors de la tempête du siècle (27–28 décembre 1999). – *Géomorphologie: relief, processus, environnement*: 127–134; doi: 10.3406/morfo.2002.1134.
- SALVADOR, P.-G., BERGER, J.-F., FONTUGNE, M. & GAUTHIER, E. (2005): Etude des enregistrements sédimentaires holocènes des paléoméandres du Rhône dans le secteur des basses terres (Ain, Isère, France). – *Quaternaire* **16** (4): 315–327.
- SANTOS, S., LUTTIKHUIZEN, P. C., CAMPOS, J., HEIP, C. H. R. & VAN DER VEER, H. W. (2011): Spatial distribution patterns of the peppery furrow shell *Scrobicularia plana* (da Costa, 1778) along the European coast: A review. – *Journal of Sea Research* **66** (3): 238–247.
- SCHÄFER, J., BLANC, G., LAPAQUELLERIE, Y., MAILLET, N., MANEUX, E. & ETCHEBER, H. (2002): Ten-year observation of the Gironde tributary fluvial system: fluxes of suspended matter, particulate organic carbon and cadmium. – *Marine Chemistry* **79** (3–4): 229–242.
- SHI, Z. & CHEN, J. Y. (1996): Morphodynamics and sediment dynamics on intertidal mudflats in China (1961–1994). – *Continental Shelf Research* **16** (15): 1909–1926.
- SIDDALL, M., ROHLING, E. J., ALMOGI-LABIN, A., HEMLEBEN, CH., MEISCHNER, D., SCHMELZER, I. & SMEED, D. A. (2003): Sea-level fluctuations during the last glacial cycle. – *Nature* **423**: 853–858.
- TANNER, W. F. (1991): Suite Statistics: The hydrodynamic evolution of the sedimental pool. – *Principles, Methods and Applications of Particle Size Analysis*: 283–292.
- THIBAUT DE CHANVALON, A., METZGER, E., MOURET, A., CESBRON, F., KNOERY, J., ROZUEL, E., LAUNEAU, P., NARDELLI, M. P., JORISSEN, F. J. & GESLIN, E. (2015): Two-dimensional distribution of living benthic foraminiferain anoxic sediment layers of an estuarine mudflat (Loire estuary, France). – *Biogeosciences* **12**: 6219–6234; doi: 10.5194/bg-12-6219-2015-supplement.
- U.S. GEOLOGICAL SURVEY (2014): Shuttle Radar Topography Mission, 1 Arc-Second scenes SRTM1N45W002V3, SRTM1N45W001V3, SRTM1N44W002V3, SRTM1N44W001V3. – Earth Resources Observation and Science (EROS) Center, <https://earthexplorer.usgs.gov/>, [01.12.2017].
- U.S. GEOLOGICAL SURVEY (2017): Landsat 8, Operational Land Imager and Thermal Infrared Sensor Scenes LC82000282017170LGN00, LC82000292017170LGN00. – Earth Resources NASA EOSDIS Land Processes DAAC, <https://earthexplorer.usgs.gov/>, [01.12.2017].

- VAN DER MEER, J. W., BENAÏSSA, A. & WEIDEMA, P. (2005): Risk-based management of flooding in the Haute Gironde. – Proceedings of the Third International Symposium on Flood Defence, Nijmegen, NL.
- YANG, B. C., DALRYMPLE, R. W. & CHUN, S. S. (2006): Sedimentation on a wavedominated, open-coast tidal flat, south-western Korea: summer tidal flat – winter shoreface. – *Sedimentology* 52 (2): 235–252.

Addresses of the authors:

Margret Mathes-Schmidt, Inst. of Neotectonics and Natural Hazards, RWTH Aachen University, Lochnerstrasse 4–20, 52056 Aachen, Germany (corresponding author).

Denis Moiriat, IRSN, Institut de Radioprotection et de Sûreté Nucléaire, BP17, 92262 Fontenay-aux-roses CEDEX, France.

Hervé Jomard, IRSN, Institut de Radioprotection et de Sûreté Nucléaire, BP17, 92262 Fontenay-aux-roses CEDEX, France.

Klaus Reicherter, Inst. of Neotectonics and Natural Hazards, RWTH Aachen University, Lochnerstrasse 4–20, 52056 Aachen, Germany.

Stéphane Baize, IRSN, Institut de Radioprotection et de Sûreté Nucléaire, BP17, 92262 Fontenay-aux-roses CEDEX, France.

Manuscript received: 31 January 2019

Revision requested: 10 April 2019

Revised version received: 21 May 2019

Manuscript accepted: 22 May 2019